Radiation Oncology

RESEARCH

Open Access

Innovative applications of visualized thermosensitive color-changing personalized boluses in post-mastectomy radiotherapy: a dosimetric analysis

Yong Wang[1†], Fujing Huang[2†], Wenmin Han[1], Jianjun Qian[1], Peifeng Zhao[1], Liesong Chen[1], Yaqun Zhu[1], Ye Tian[1] and Yanze Sun[1*]

Abstract

Background and purpose To explore the feasibility and advantages of the visualized thermosensitive color-changing personalized bolus in post-mastectomy radiotherapy (PMRT).

Materials and methods Forty PMRT patients (June 2023–June 2024) were randomized into two groups. Group A (experimental group, 20 patients) underwent two CT scans: A_1 (without compensator) and A_2 (with the visualized thermosensitive color-changing personalized bolus), followed by treatment with the thermosensitive color-changing personalized bolus. Group B (control group, 20 patients) also underwent two CT scans: B_1 (without bolus) and B_2 (with a conventional commercial bolus), followed by treatment with the commercial bolus. Treatment plans were generated for virtual bolus (A_1-Plan, B_1-Plan) and real bolus (A_2-Plan, B_2-Plan). A_3-Plan (A_1-Plan applied to thermosensitive bolus treatment) and B_2-Plan (B_1-Plan applied to commercial bolus treatment) were compared to evaluate dosimetric differences in target volumes, organs at risk (OARs), and skin toxicity.

Results In Group A, A_1-Plan and A_2-Plan showed no significant differences in OAR doses (e.g., ipsilateral lung, heart, contralateral breast, skin D_{max}/D_{mean}) or target metrics (V_{50Gy}, D_{max}, homogeneity index (HI), conformity index (CI), monitor units (MU)). A_3-Plan compared to A_1-Plan had minor differences in target coverage (94.05% vs. 95.14%), HI (0.148 vs. 0.147), and CI (0.83 vs. 0.84). In Group B, B_2-Plan had significantly reduced target coverage (89.9% vs. 95%), homogeneity (0.153 vs. 0.136), and conformity (0.817 vs. 0.810) compared to B_1-Plan, attributed to air gaps from the commercial bolus. The thermosensitive color-changing personalized bolus had better skin adherence, significantly reduced air cavity volumes (3833 mm^3 vs. 21498 mm^3), and maintained equivalent dosimetric performance to virtual boluses. Skin toxicity was Grade I in all patients without differences between groups.

[†]Yong Wang and Fujing Huang contributed equally and are joint first authors.

*Correspondence:
Yanze Sun
syzkk0109@163.com

Full list of author information is available at the end of the article

Conclusions The visualized thermosensitive color-changing personalized bolus demonstrated superior skin adherence, smaller air gaps, and better positional reproducibility compared to commercial boluses. Its dosimetric performance was consistent with virtual bolus plans, ensuring target coverage and OAR protection without increased skin toxicity. These findings support its clinical application in PMRT.

Keywords Breast Cancer, Post-Mastectomy radiotherapy, Thermosensitive, Color-changing, Bolus

Introduction

Postoperative radiotherapy (RT) following radical mastectomy for breast cancer plays a vital role in reducing the risk of locoregional recurrence and improving overall survival. Clinical trials and meta-analyses have consistently demonstrated the benefits of RT in eradicating residual microscopic disease and preventing tumor relapse, particularly in patients with high-risk features such as lymph node involvement [1, 2]. Advances in radiotherapy techniques, including intensity-modulated radiotherapy (IMRT) and image-guided radiotherapy (IGRT), have enabled precise targeting of affected tissues while minimizing exposure to surrounding organs, thereby reducing treatment-related complications [3, 4]. Additionally, clinical guidelines emphasize personalized RT planning based on tumor characteristics and individual patient anatomy, ensuring optimal therapeutic outcomes [5]. Long-term follow-up studies further underscore the sustained benefits of postoperative RT in improving disease-free and overall survival, establishing its role as a cornerstone of multidisciplinary breast cancer management [6].

In postoperative radiotherapy for breast cancer, the target volume often lies close to the skin surface, necessitating specific considerations for dose distribution. Due to the dose build-up effect, achieving adequate superficial dose coverage requires the use of boluses to bridge the build-up region and ensure effective treatment. Traditional boluses, such as bolus materials like tissue-equivalent gels or solid sheets, have been widely utilized; however, their application can be inconsistent, potentially leading to dose heterogeneity [7, 8]. Recent advances in three-dimensional (3D) printing have introduced patient-specific boluses, which conform precisely to the unique contours of the patient's anatomy, enhancing dose uniformity and reducing air gaps [9, 10]. These 3D-printed boluses are particularly advantageous for complex or irregular surfaces, providing improved treatment reproducibility compared to conventional boluses [11, 12]. Despite these benefits, challenges such as increased production time and cost remain barriers to widespread adoption. Ongoing research seeks to optimize materials and manufacturing processes to overcome these limitations while maintaining clinical efficacy [13–15].

Thermochromic materials are commonly seen in daily life, with a wide range of applications such as baby bath tubs and thermos cups. These products leverage the thermochromic properties to visually indicate temperature changes, providing users with convenience and safety. However, the application of this technology in the medical field, particularly in compensator membranes for post-mastectomy breast cancer patients, has not yet been reported in the literature. The visualized thermosensitive color-changing personalized bolus represents an innovative advancement in postoperative radiotherapy for breast cancer. Composed of medical-grade silicone infused with thermosensitive particles, this membrane leverages color changes to provide real-time visualization of cavity positions and surface areas during treatment. Its ability to be customized to individual patient anatomy ensures precise adaptation to complex surfaces, reducing the risk of air gaps and enhancing dose conformity. This personalized approach addresses limitations of traditional boluses, such as variability in fit and inconsistency in dose distribution. Additional benefits include improved workflow efficiency, as the real-time color feedback facilitates rapid adjustments during treatment setup. Moreover, preliminary studies indicate that the thermosensitive color-changing personalized bolus reduces radiation-induced skin toxicity by enabling more even dose coverage while minimizing hotspots in the build-up region. These advantages highlight the potential of this novel material to improve clinical outcomes and patient comfort in radiotherapy.

This study focuses on evaluating the application of the visualized thermosensitive personalized bolus in postoperative radiotherapy for breast cancer. By comparing its performance with that of commercial boluses, we aim to assess differences in dosimetric outcomes and skin toxicity responses. The thermosensitive color-changing personalized bolus's ability to conform precisely to patient anatomy and provide real-time visualization of treatment areas offers potential advantages in dose distribution uniformity and reduction of hotspots. Furthermore, the study examines its role in mitigating radiation-induced skin toxicity, a common complication in breast cancer radiotherapy. Through this comparative analysis, we aim to validate the feasibility and clinical utility of the visualized thermosensitive color-changing personalized bolus as an innovative tool in enhancing treatment accuracy and patient outcomes. The findings are expected to provide insights into integrating this novel technology into routine radiotherapy practices.

Materials and methods

Patient selection and thermosensitive Color-changing personalized bolus fabrication

This study included 40 breast cancer patients who underwent radical mastectomy and were treated in the Department of Radiation Oncology at the Second Affiliated Hospital of Soochow University from June 2023 to June 2024. The median age of the participants was 57 years (range: 34–74 years). Written informed consent was obtained from all patients, and the study was approved by our local ethics committee (JD-Li-2022-023-01).

The visualized thermosensitive color-changing personalized bolus was fabricated using medical-grade low-hardness silicone, selected for its physical density (1.06 g/cm^3), closely resembling that of the human chest wall skin. Thermosensitive color-changing particles were integrated into the material, enabling real-time color variation based on the temperature of the contacted object. The threshold temperature for color change was adjustable to meet clinical requirements. The compensator membrane featured a multi-layered design to optimize hardness, viscosity, and toughness, ensuring both ideal physical properties and excellent adherence to the skin surface.

Positioning and CT image acquisition

All patients were positioned in a supine posture using a breast support frame for immobilization, with both arms abducted and raised overhead. Computed tomography (CT) imaging was performed using a GE RT 590 16-slice large-bore CT scanner. Patients were randomly divided into two groups (Group A and Group B) using the labeling method. For Group A, each patient underwent two CT scans (A_1 and A_2). The A_1 scan was performed without a bolus, using standard CT contrast-enhanced imaging. The A_2 scan was conducted with a 0.3 cm-thick visualized thermosensitive color-changing personalized bolus applied to the chest wall, which was customized and trimmed to fit the patient's anatomy. Similarly, Group B patients also underwent two CT scans (B_1 and B_2). The B_1 scan was performed without a bolus, and the B_2 scan was conducted with a 0.3 cm-thick conventional commercial bolus (silicone material, 30 cm × 30 cm) applied to the chest wall.

Target delineation and treatment planning

Target volumes and organs at risk (OARs) were delineated on the A_1 and B_1 images by clinical physicians using MIM software. Target volumes included the supraclavicular region and chest wall, while OARs included both lungs, the heart, the contralateral breast, and the spinal cord. These delineated structures were then transferred to the A_2 and B_2 images via image fusion. All images and structures were imported into the Pinnacle treatment planning system (Philips, Version 9.8). The prescribed dose for the planning target volume (PTV) was 50 Gy, delivered in 2 Gy fractions over 25 fraction. Planning requirements included $V_{50Gy} \geq 95\%$, $D_{max} < 60$ Gy; ipsilateral lung $V_{20Gy} < 30\%$; mean heart dose (D_{mean}) < 6 Gy for left-sided targets and < 4 Gy for right-sided targets.

An 8-field intensity-modulated radiotherapy (IMRT) plan was created for each patient, with beam angles primarily along tangential directions. For left-sided breast cancer, tangential beam angles ranged from 300° to 345° and 100° to 135°, with an additional beam at 355°. For right-sided breast cancer, tangential beam angles ranged from 25° to 60° and 220° to 265°, with an additional beam at 5°. Beam angles were slightly adjusted based on the target shape to avoid beam cross-pass.

In the radiotherapy planning system, a virtual bolus was added to A_1 images to create a clinically optimized plan, referred to as A_1-Plan (the ideal scenario). For A_2, a clinically acceptable plan was created with thermosensitive color-changing personalized bolus, referred to as A_2-Plan (thermosensitive bolus plan). Both plans used the same beam angles and target optimization functions. A_1-Plan was then transferred to A_2, resulting in A_3-Plan (simulating the scenario where the plan was designed with a virtual bolus but treated with a thermosensitive bolus). Similarly, a virtual bolus was added to B_1 to create a clinically optimized plan, referred to as B_1-Plan (ideal scenario), and B_1-Plan was transferred to B_2, resulting in B_2-Plan (a plan designed with a virtual bolus but treated with a commercial bolus).

In current clinical practice, it is common to design plans using a virtual bolus and perform treatment using a commercial bolus. Therefore, in this study, no separate plan was created for B_2. A comparison between A_1-Plan and A_2-Plan aims to illustrate the differences between plans using a virtual bolus versus a thermosensitive color-changing personalized bolus. A comparison between A_1-Plan and A_3-Plan aims to assess the magnitude of the differences if, similar to the B-group plans, a virtual compensator is used for planning while a thermosensitive bolus is used for treatment. Finally, a comparison between B_1-Plan and B_2-Plan evaluates the differences in the current clinical practice of designing plans with a virtual bolus and treating with a commercial bolus.

Dosimetric comparisons

Target dose parameters included $V_{50\%}$, D_{max}, homogeneity index (HI), and conformity index (CI). CI was calculated as $CI = TV_{50Gy}/V_{50Gy}$, and HI as $HI=(D_{2\%}-D_{98\%})/D_{98\%}$, where TV_{50Gy} and V_{50Gy} represent the volume of the target and the body encompassed by the 50 Gy dose line, respectively, and $D_{x\%}$ indicates the dose covering x% of the target volume. Skin evaluation parameters included the maximum dose (D_{max}) and mean dose

(D_{mean}) within the skin of the chest wall target area. Dose parameters for normal tissues included ipsilateral lung V_{5Gy}, V_{10Gy}, and V_{20Gy}, as well as D_{mean} for the heart and contralateral breast.

Radiotherapy plan implementation and verification

Following clinical review, the approved treatment plans were transferred via the network to the Elekta Synergy linear accelerator for delivery, using 6 MV X-rays. Plan verification was performed for all patients during their first treatment fraction using a two-dimensional flat-panel detector (Sun Nuclear, MapCheck2, USA). The detector was placed horizontally on the treatment couch, and all beam fields were normalized to a 0° gantry angle to analyze individual field dose distributions. Treatment was initiated only if the Gamma passing rate reached 95% or higher (criteria: 3 mm distance-to-agreement, 2% dose difference). Cone-beam computed tomography (CBCT) was used for positional verification during the initial treatment fraction and weekly thereafter.

During treatment, Group A patients had a 0.3 cm thick visualized thermosensitive color-changing personalized bolus applied to the chest wall, while Group B patients used a 0.3 cm thick commercial bolus. These boluses were applied to ensure consistent dose delivery in accordance with the treatment plan.

Measurement of air gaps between bolus and skin

CBCT images from both patient groups were transferred to the Monaco 5.0 software for analysis. Using threshold segmentation, the air cavity data between the patient's skin surface and the bolus were extracted. A three-dimensional (3D) model of the air gap was reconstructed for each patient. The 3D model volumes of the air cavities were measured to quantify the total air gap volume for each patient. Additionally, the distance from the bolus to the skin surface was analyzed, and the location of the maximum gap distance was identified and measured. This analysis enabled a detailed evaluation of the fit and conformity of the bolus to the patient's anatomy.

Assessment of skin reactions

Skin toxicity during and after post-mastectomy radiotherapy (PMRT) was evaluated based on the Radiation Therapy Oncology Group (RTOG) classification for radiation-induced skin injury. The grading criteria were as follows: Grade 1, mild erythema, dry desquamation, or both; Grade 2, moderate erythema or patchy moist desquamation; Grade 3, confluent moist desquamation, punctate edema, and tenderness; and Grade 4, necrosis, ulceration, or bleeding. Skin toxicity grades were assessed by two to three radiation therapy personnel to ensure accuracy and consistency. Patients underwent weekly assessments of skin reactions from the start of radiotherapy until four weeks after completing PMRT. During the treatment period, patients were advised by their physicians to keep the irradiated chest wall dry, minimize friction, and use a radiation protective spray as needed to manage and prevent skin irritation.

Statistical analysis

Statistical analysis was performed using SPSS software (version 19.0). Data that followed a normal distribution were presented as mean ± standard deviation ($\bar{x} \pm s$). Paired sample t-tests were used to analyze the results for tumor target volumes and organs at risk (OARs). Pearson correlation analysis was conducted to assess the relationship between body mass index (BMI), chest wall flatness, and air cavity volume. A P-value of < 0.05 was considered statistically significant.

Results

Effectiveness of the visualized thermosensitive color-changing personalized bolus

The application of the visualized thermosensitive color-changing personalized bolus demonstrated its effectiveness in ensuring proper adherence to the skin surface. Figure 1 illustrates the results for a patient following radical mastectomy for breast cancer. Initially, incomplete adherence was observed in areas such as the surgical incision site, skin folds, and depressions. These regions were indicated by the membrane turning purple, signaling inadequate contact. After fine-tuning the position and contour of the bolus to achieve complete adherence to the skin, the purple color disappeared, and the membrane transitioned to a transparent state, confirming proper placement and fit.

Comparison of target dose parameters

The comparison of target dose parameters for the two groups is summarized in Table 1. In Group A, no significant differences were observed between A_1-Plan and A_2-Plan in terms of the target volume encompassed by the prescription dose (V_{50Gy}), maximum dose (D_{max}), homogeneity index (HI), conformity index (CI), and monitor units (MU). The results indicate that the plans designed with or without the visualized thermosensitive color-changing personalized bolus showed similar dosimetric characteristics. When comparing A_3-Plan (a plan designed with a virtual bolus and treated with the visualized thermosensitive color-changing personalized bolus) to A_1-Plan, statistically significant differences were found in V_{50Gy}, D_{max}, HI, and CI. However, the differences were minimal, suggesting that the use of a virtual bolus for planning and the visualized thermosensitive color-changing personalized bolus for treatment did not substantially impact target coverage, conformity, or homogeneity.

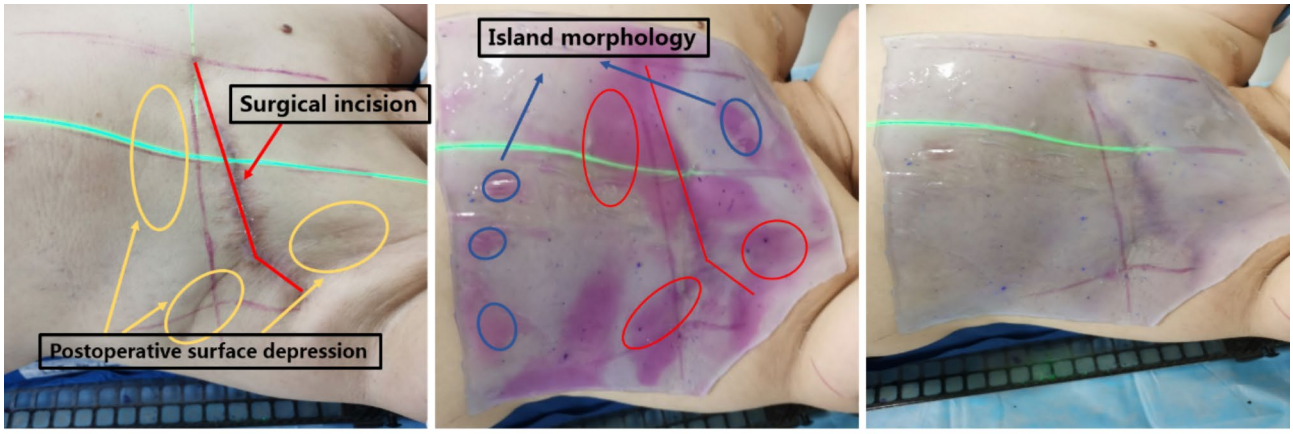

Fig. 1 Application Effect of the Visualized Thermosensitive color-changing personalized bolus. **A** Surface morphology of the chest wall in a post-mastectomy patient prior to the application of the bolus during CT simulation. **B** Initial placement of the visualized thermosensitive color-changing personalized bolus, showing a purple color in areas of incomplete contact, such as scars and folds. **C** Final placement of the visualized thermosensitive color-changing personalized bolus, demonstrating complete adherence to the skin surface, with the purple color disappearing.

Table 1 Comparison of target dose parameters for groups A and B

		V_{50Gy}(%)	D_{max} (cGy)	HI	CI	MU
Group A	A1-plan	95.14 ± 1.89	5644.80 ± 47.07	0.15 ± 0.031	0.84 ± 0.053	826.00 ± 27.43
	A2-Plan	94.93 ± 1.57	5639.80 ± 46.37	0.15 ± 0.031	0.84 ± 0.055	786.45 ± 146.63
	A3-Plan	94.05 ± 2.21	5665.40 ± 45.30	0.15 ± 0.006	0.83 ± 0.055	826.00 ± 27.43
	t-value	-1.754 [a]	-0.402 [a]	-0.082 [a]	0.893 [a]	-1.403 [a]
		5.036 [b]	-5.075 [b]	-3.387 [b]	2.529 [b]	——
	P-value	0.096 [a]	0.692 [a]	0.936 [a]	0.383 [a]	0.177 [a]
		0.000[b]	0.000[b]	0.003[b]	0.020[b]	——
Group B	B1-Plan	95.06 ± 1.60	5645 ± 50.06	0.14 ± 0.022	0.81 ± 0.042	769.95 ± 137.87
	B2-Plan	89.90 ± 2.45	5632.65 ± 45.68	0.16 ± 0.028	0.82 ± 0.041	769.95 ± 137.87
	t-value	8.490	2.994	-4.930	-1.450	——
	P-value	0.000	0.007	0.000	0.160	——

Note: a indicates the comparison between A1-Plan and A2-Plan; b indicates the comparison between A1-Plan and A3-Plan; "—" indicates no data available

In Group B, significant differences were found between B_1-Plan and B_2-Plan for V_{50Gy}, D_{max}, and HI. The results indicate that plans designed with a virtual bolus but treated with a commercial bolus showed reduced target coverage, conformity, and homogeneity. Moreover, the prescription dose coverage, HI, and CI of A_3-Plan with the visualized thermosensitive color-changing personalized bolus were notably superior to those of B_2-Plan with the commercial bolus in Group B. This highlights the advantage of using the visualized thermosensitive color-changing personalized bolus over conventional commercial bolus options in maintaining dosimetric accuracy.

Comparison of dose to organs at risk

The comparison of dose to organs at risk (OARs) for the two groups is presented in Table 2. In Group A, no significant differences were observed between A_1-Plan and A_2-Plan in the ipsilateral lung volumes receiving 5 Gy (V_{5Gy}), 10 Gy (V_{10Gy}), and 20 Gy (V_{20Gy}); the maximum dose (D_{max}) and mean dose (D_{mean}) to the chest wall skin; the mean heart dose (D_{mean}); and the mean dose to the contralateral breast (D_{mean}). When comparing A_3-Plan with A_1-Plan, a slight increase in chest wall skin dose was observed, but the difference was minor and clinically acceptable.

In Group B, comparisons between B_1-Plan and B_2-Plan showed similar results for ipsilateral lung V_{5Gy}, V_{10Gy}, and V_{20Gy}, chest wall skin D_{max} and D_{mean}, heart D_{mean}, and contralateral breast D_{mean}. Notably, the use of the commercial bolus resulted in a slight reduction in the average skin dose, though the differences were not statistically significant.

Adherence of bolus to skin

The air cavity volumes for all patients were delineated using threshold segmentation. The mean air cavity volume for the visualized thermosensitive personalized color-changing personalized bolus was 3833 ± 3185 mm^3, with a mean maximum air gap distance of 3.6 ± 1.7 mm. In contrast, the commercial bolus had a mean air cavity

Table 2 Comparison of OAR dose parameters for groups A and B

		Ipsilateral (%)			Skin (cGy)		Heart (cGy)	Contralateral breast (cGy)
		V_{5Gy}	V_{10Gy}	V_{20Gy}	D_{max}	D_{mean}	D_{mean}	D_{mean}
Group A	A1-Plan	51.75 ± 3.23	36.81 ± 2.18	26.45 ± 1.89	5596.7 ± 17.41	5108.83 ± 49.56	623.62 ± 24.80	245.64 ± 122.85
	A2-Plan	51.78 ± 3.41	36.82 ± 2.08	26.33 ± 1.91	5598.1 ± 20.8	5111.06 ± 58.57	621.42 ± 27.06	238.74 ± 113.83
	A3-Plan	51.82 ± 5.07	36.82 ± 3.28	26.41 ± 1.89	5674.3 ± 97.33	5153.6 ± 81.99	627.45 ± 215.00	247.35 ± 120.96
	t-value	0.088 [a]	0.045 [a]	-0.914 [a]	0.055 [a]	0.226 [a]	-0.121 [a]	-1.21 [a]
		-0.678 [b]	-0.106 [b]	2.021 [b]	-4.723 [b]	-2.791 [b]	-6.056 [b]	-0.658 [b]
	P-value	0.931 [a]	0.964 [a]	0.372 [a]	0.957 [a]	0.823 [a]	0.906 [a]	0.241 [a]
		0.396[b]	0.916[b]	0.058[b]	0.000[b]	0.012[b]	0.000[b]	0.518[b]
Group B	B1-Plan	53.02 ± 5.50	38.98 ± 3.67	27.27 ± 1.66	5597.3 ± 71.15	5118.42 ± 31.89	647.14 ± 157.29	220.67 ± 83.05
	B2-Plan	53.07 ± 5.51	38.97 ± 3.71	27.20 ± 1.67	5627.1 ± 130.57	5048.17 ± 89.24	650.98 ± 166.91	220.31 ± 84.42
	t-value	-0.525	0.274	2.467	-1.556	3.236	-0.873	0.244
	P-value	0.61	0.787	0.023	0.136	0.004	0.403	0.81

Note: a indicates the comparison between A1-Plan and A2-Plan; b indicates the comparison between A1-Plan and A3-Plan; "—" indicates no data available

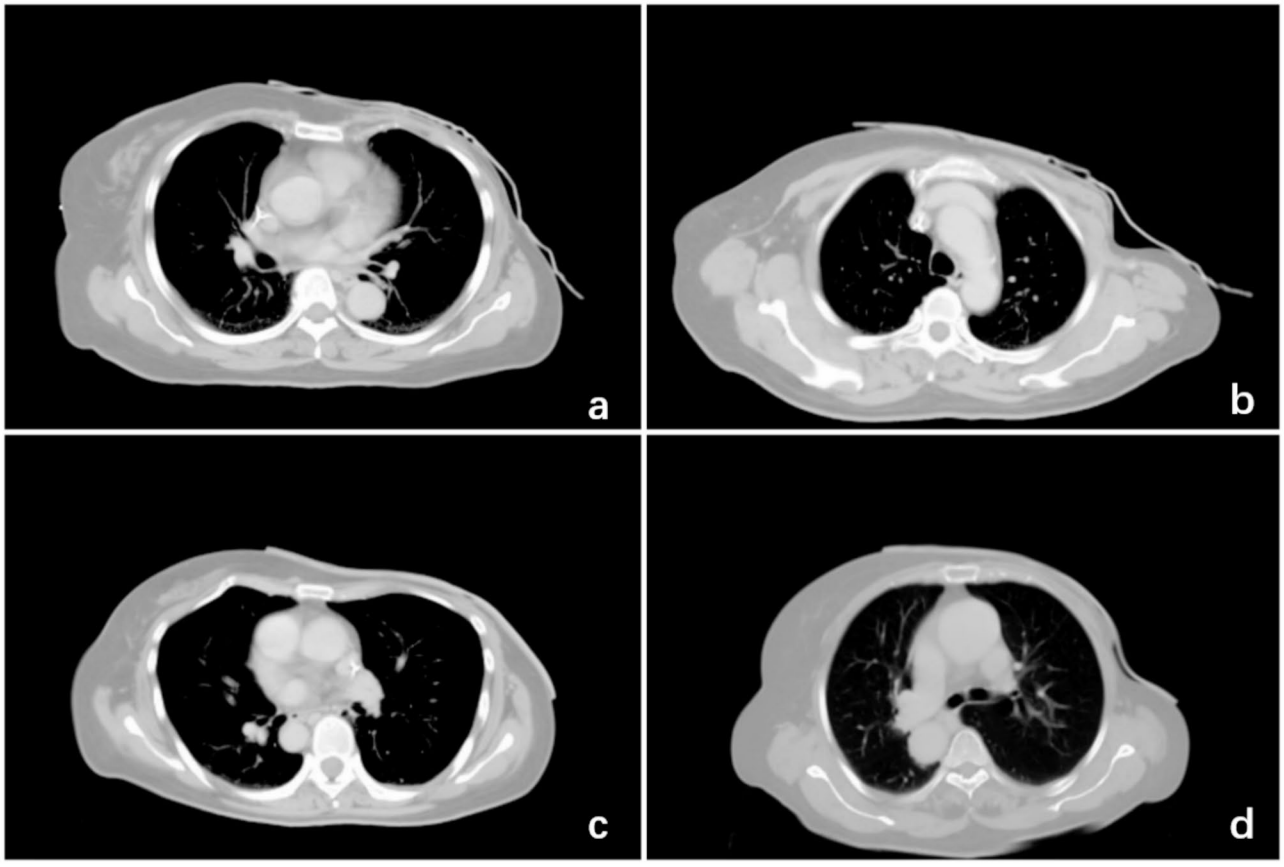

Fig. 2 Application of Conventional Commercial Bolus and Visualized Thermosensitive Color-changing Personalized Bolus in Breast Cancer Patients. **a** and **c** Patients with relatively flat chest wall contours. **b** and **d** Patients with steeper chest wall contours. **c** and **d**: The visualized thermosensitive color-changing personalized bolus shows better adherence to the skin compared to the conventional commercial bolus used in **a** and **b**

volume of 21,498 ± 6863 mm^3 and a mean maximum air gap distance of 9.7 ± 4.0 mm. Both metrics showed statistically significant differences between the two types of boluses ($P < 0.001$). Pearson correlation analysis revealed no significant correlations between body mass index (BMI), chest wall flatness, and either air cavity volume or maximum air gap distance.

Figure 2 illustrates the clinical application of the conventional and visualized thermosensitive color-changing personalized boluses. Regardless of whether patients had relatively flat or steep chest wall contours, the visualized thermosensitive color-changing personalized bolus demonstrated superior adherence to the skin surface compared to the conventional commercial bolus.

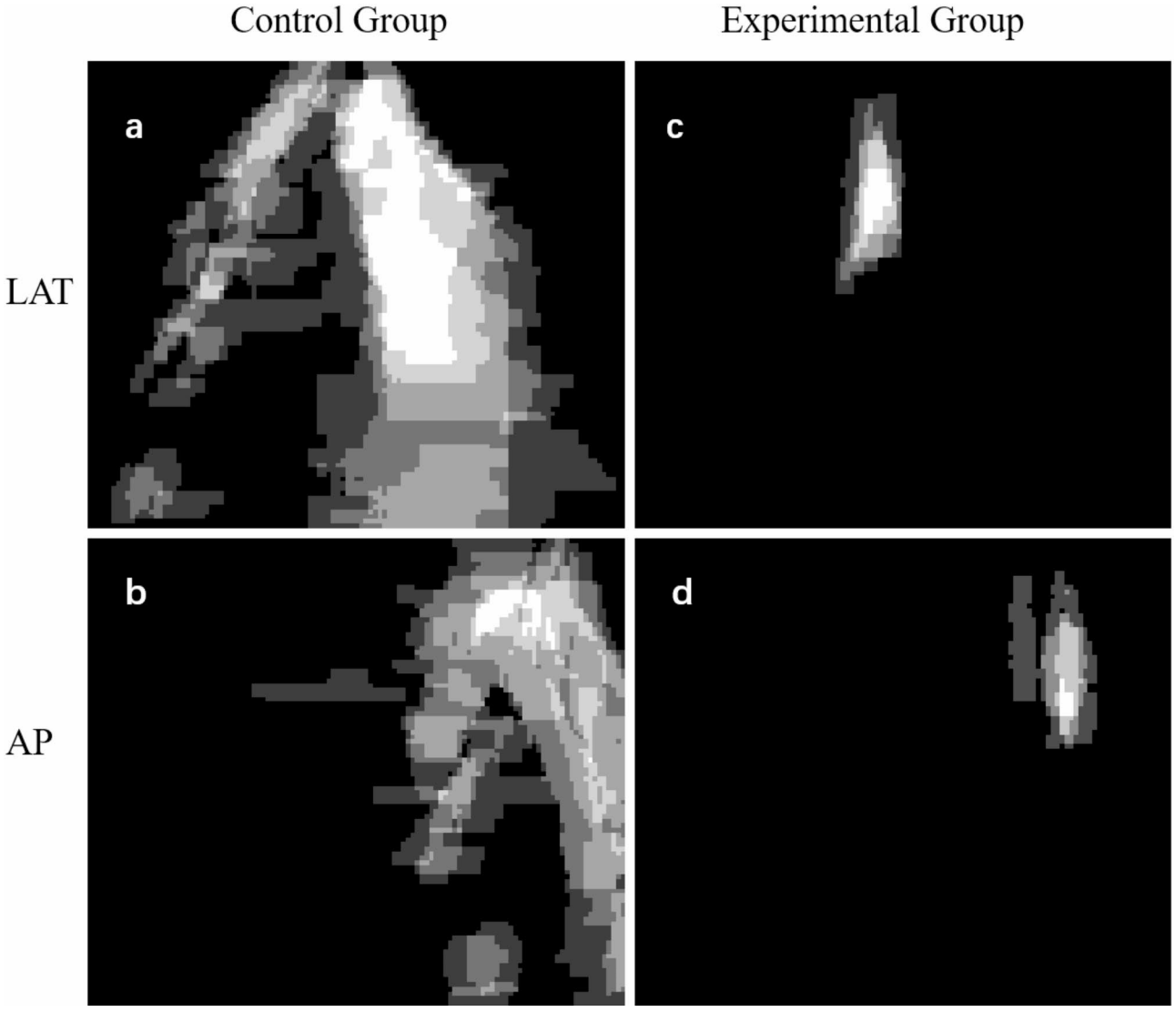

Fig. 3 Grayscale overlay image of the cavity region. Figures **a** and **b** represent the control group with the commercial bolus, showing widespread grayscale regions, indicating larger cavity volumes. Figures **c** and **d** represent the experimental group with the visualized thermosensitive color-changing personalized bolus, showing smaller grayscale regions and fewer cavity areas

In the Monaco planning system, after delineating the cavity for each patient based on CBCT, 0° DR anterior projections (AP) and 90° DR lateral projections (LAT) were reconstructed separately. All images were processed to a unified pixel size of 115 × 100 for Dice coefficient calculations. The Dice coefficient for the commercial bolus was 0.61 ± 0.12, while that for the visualized thermosensitive color-changing personalized bolus was 0.93 ± 0.06.

Figure 3 shows grayscale overlay images of the cavity region. After overlaying the grayscale of anterior and lateral CBCT images throughout the entire treatment process, non-black areas represent the cavity region, and the larger the black area, the smaller the cavity volume. The whiter the area, the more overlap in the cavity region, indicating greater cavity stability. For the commercial bolus, the cavity region was concentrated around the affected side's mid-axillary line and the surgical incision, with the mid-axillary line cavity likely resulting from poor adhesion due to membrane sagging. In contrast, for the visualized thermosensitive color-changing personalized bolus, the cavity region was concentrated near the postoperative incision.

Skin toxicity reactions

Among the 40 enrolled patients, all had the bolus removed after 20 treatment fractions to ensure adequate skin dose coverage. In both the experimental group (visualized thermosensitive color-changing personalized bolus) and the control group (commercial bolus), all observed skin toxicity reactions were classified as Grade

I, with no occurrences of Grade II or higher skin reactions during or after treatment.

Discussion

This study aimed to evaluate the dosimetric characteristics, efficacy, and safety of the visualized thermosensitive color-changing personalized bolus in patients undergoing post-mastectomy radiotherapy (PMRT). The results demonstrate that the application of this membrane ensures adequate skin dose coverage, uniform chest wall dose distribution, effective protection of critical organs, and acceptable levels of skin toxicity. These findings highlight the membrane's practicality and safety, offering a more precise and effective radiotherapy strategy for PMRT patients. Its innovative features, including superior skin adherence and real-time visualization, make it a valuable tool for enhancing treatment accuracy and clinical outcomes in this patient population.

The visualized thermosensitive color-changing personalized bolus is primarily composed of medical-grade silicone combined with thermosensitive microcapsules, with a density of 1.06 g/cm^3. The thermosensitive microcapsules (micron-scale) are fabricated using an electron transfer-based organic compound system. When the object temperature reaches a specific threshold, electron transfer occurs within the microcapsules, resulting in a reversible color change—a safe and non-toxic physical reaction. This color-changing material not only exhibits vivid color but also allows a unique transition from "colored to colorless," a capability absent in heavy metal double salt complexes and liquid crystal-based thermochromic materials. By observing these color changes, the position and size of air cavities can be monitored in real time. During patient setup, therapists can efficiently expel air from the cavities, ensuring complete membrane adherence as indicated by the transition from purple to transparent.

Compared to conventional commercial bolus, the thermosensitive color-changing personalized bolus reduced the air cavity volume by nearly one-seventh and the maximum air gap distance by approximately one-third. This performance was even superior to air cavity volumes reported for 3D-printed compensator membranes in the literature [16, 17]. Additionally, weekly CBCT scans throughout the radiotherapy course demonstrated good reproducibility and consistency of the thermosensitive membrane. As shown in Fig. 2, the thermosensitive personalized bolus provided better adherence to the skin surface than conventional boluses, regardless of whether the chest wall contour was relatively flat or steep.

In the clinical application of bolus for post-mastectomy radiotherapy (PMRT) patients, it is common to design treatment plans using virtual bolus while employing conventional commercial bolus during actual therapy. This practice often leads to discrepancies between planned and delivered doses. In our study, significant differences were observed in target dose parameters between the two plans in the control group (Group B). Specifically, the actual treatment plans exhibited reduced target coverage and homogeneity. The presence of air gaps resulted in a decreased mean skin dose to the chest wall ($P = 0.004$), aligning with findings from other studies that have reported dosimetric differences due to the method of bolus application [18]. The virtual bolus in B_1-Plan was designed to conform closely to the patient's surface, whereas the conventional commercial bolus used during treatment had inherent rigidity, creating gaps between the bolus and the skin surface, leading to deviations from the ideal dose distribution. Multiple studies have demonstrated that air gaps can adversely affect target dose distribution, reducing the expected dose and uniformity.

In contrast, the experimental group utilizing the thermosensitive color-changing personalized bolus exhibited superior conformity. Comparisons between plans with the thermosensitive bolus and their corresponding virtual bolus plans revealed no significant differences in target dose coverage, homogeneity, conformity, or doses to organs at risk. When the virtual bolus plan was applied to the visualized thermosensitive color-changing personalized bolus, the differences in target dose coverage, homogeneity, and conformity were minimal, indicating good consistency. This performance was notably better than that of the conventional commercial bolus.

In this study, all 40 enrolled patients exhibited Grade 1 skin reactions, with no occurrences of higher-grade skin toxicity. The frequency of bolus application is a critical factor influencing target coverage and skin dose. Dahn et al. reported that daily bolus use can lead to Grade 3 skin toxicity rates ranging from 45 to 88% [19]. Another study indicated that applying the bolus for 15 to 20 out of 25 fractions in post-mastectomy three-dimensional conformal radiotherapy (3D-CRT) effectively balances target and skin doses [20]. In our research, all patients had the bolus removed after 20 fractions to ensure adequate skin dose. The visualized thermosensitive color-changing personalized bolus used is made of silicone material, which is considered safer and more environmentally friendly compared to traditional materials [21]. Additionally, patient education emphasizing the reduction of skin friction, maintaining dry chest wall skin, and the use of radiation protective sprays played a significant role in minimizing skin toxicity during radiotherapy.

Although visualized thermosensitive color-changing personalized bolus have clear advantages, it is still necessary to measure the actual dose on the patient's skin surface, which is a limitation of this paper. The next step is to compare the measurements of commercial bolus and visualized thermosensitive color-changing personalized

bolus using thermoluminescence dosimetry (TLD) or film dosimeters. The research methods of O.V. Gul et al. [22] and H. Demir et al. [23] have provided valuable reference and guidance for the next phase of this study.

Conclusion

In summary, the visualized thermosensitive color-changing personalized bolus demonstrates excellent adherence to the skin, helping to overcome the dosimetric discrepancies caused by unnecessary air gaps in breast cancer radiotherapy. This innovation enhances patient comfort, allows for personalized tailoring to individual anatomical features, and offers low-cost and visual feedback advantages, significantly reducing uncertainties in daily patient positioning. The membrane achieves target dose coverage, homogeneity, and organ-at-risk protection comparable to the ideal virtual bolus, without increasing skin toxicity. Given these advantages, the visualized thermosensitive color-changing personalized bolus presents a viable alternative to conventional commercial bolus and holds significant promise for clinical application and widespread adoption in PMRT patients.

Acknowledgements
Not applicable.

Author contributions
Yong Wang and Fujing Huang carried out the data collection, and statistical analysis and drafted the manuscript. Wenmin Han, Jianjun Qian and Peifeng Zhao participated in the data collection and statistical analysis. Yaqun Zhu, Liesong Chen, and Ye Tian evaluated the skin toxicity. Yanze Sun revised and finally approved the manuscript. All authors contributed to the article and approved the submitted version.

Funding
The author(s) disclosed receipt of the following financial support for the research, authorship, and/or publication of this article: This work was supported by Key Medical Discipline Construction Unit of Jiangsu Province for the 14th Five-year plan (JSDW202236) and The Suzhou Science and Technology Program (Medical and Health Technology Innovation) Project (SKY2022167).

Data availability
No datasets were generated or analysed during the current study.

Declarations

Ethics approval and consent to participate
This study was approved by the Ethical review Board for research of Second Affiliated Hospital of Soochow University. All patients have signed informed consent.

Consent for publication
Written informed concent for publication was obtained from all authors.

Competing interests
The authors declare no competing interests.

Author details
[1]Department of Radiotherapy Oncology, the Second Affiliated Hospital of Soochow University, Institute of Radiotherapy Oncology, Soochow University, Suzhou Key Laboratory for Radiation Oncology, Suzhou 215004, China
[2]Affiliated Hospital, Shandong University of Traditional Chinese Medicine, Jinan 250014, China

Received: 5 January 2025 / Accepted: 13 March 2025
Published online: 27 March 2025

References

1. Early Breast Cancer Trialists' Collaborative Group (EBCTCG), Darby S, McGale P, et al. Effect of radiotherapy after breast-conserving surgery on 10-year recurrence and 15-year breast cancer death: meta-analysis of individual patient data for 10,801 women in 17 randomised trials. Lancet. 2011;378(9804):1707–16. https://doi.org/10.1016/S0140-6736(11)61629-2
2. Dahn HM, Boersma LJ, de Ruysscher D, et al. The use of bolus in postmastectomy radiation therapy for breast cancer: A systematic review. Crit Rev Oncol Hematol. 2021;163:103391. https://doi.org/10.1016/j.critrevonc.2021.103391
3. Chang JS, Chang JH, Kim N, Kim YB, Shin KH, Kim K. Intensity modulated radiotherapy and volumetric modulated Arc therapy in the treatment of breast cancer: an updated review. J Breast Cancer. 2022;25(5):349–65. https://doi.org/10.4048/jbc.2022.25.e37
4. Cheng HW, Chang CC, Shiau AC, Wang MH, Tsai JT. Dosimetric comparison of helical tomotherapy, volumetric-modulated Arc therapy, intensity-modulated radiotherapy, and field-in-field technique for synchronous bilateral breast cancer. Med Dosim. 2020;45(3):271–7. https://doi.org/10.1016/j.meddos.2020.01.006
5. Bevers TB, Niell BL, Baker JL, et al. NCCN Guidelines® insights: breast cancer screening and diagnosis, version 1.2023. J Natl Compr Canc Netw. 2023;21(9):900–9. https://doi.org/10.6004/jnccn.2023.0046
6. Yang SX, Polley EC. Systemic treatment and radiotherapy, breast cancer subtypes, and survival after long-term clinical follow-up. Breast Cancer Res Treat. 2019;175:287–95. https://doi.org/10.1007/s10549-019-05142-x
7. Oliver PAK, Monajemi TT. Skin dose in chest wall radiotherapy with Bolus: a Monte Carlo study. Phys Med Biol. 2020;65(15):155016. https://doi.org/10.1088/1361-6560/ab95dc
8. Al-Rahbi ZS, Cutajar DL, Metcalfe P, Rosenfeld AB. Dosimetric effects of brass mesh bolus on skin dose and dose at depth for postmastectomy chest wall irradiation. Phys Med. 2018;54:84–93. https://doi.org/10.1016/j.ejmp.2018.09.009
9. McCallum S, Maresse S, Fearns P. Evaluating 3D-printed bolus compared to conventional bolus types used in external beam radiation therapy. Curr Med Imaging. 2021;17(7):820–31. https://doi.org/10.2174/1573405617666210202114336
10. Chatchumnan N, Kingkaew S, Aumnate C, Sanghangthum T. Development and dosimetric verification of 3D customized bolus in head and neck radiotherapy. J Radiat Res. 2022;63(3):428–34. https://doi.org/10.1093/jrr/rrac013
11. Pollmann S, Toussaint A, Flentje M, Wegener S, Lewitzki V. Dosimetric evaluation of commercially available flat vs. Self-Produced 3D-Conformal silicone boluses for the head and neck region. Front Oncol. 2022;12:881439. https://doi.org/10.3389/fonc.2022.881439
12. Kong Y, Yan T, Sun Y, et al. A dosimetric study on the use of 3D-printed customized boluses in photon therapy: A hydrogel and silica gel study. J Appl Clin Med Phys. 2019;20(1):348–55. https://doi.org/10.1002/acm2.12489
13. Sharma R, Malviya R, Sundram S, et al. Advancement in 3D printable materials for the management of cancer: A new era of materialistic approach for the treatment of cancer[J]. J Drug Deliv Sci Technol. 2024;106064. https://doi.org/10.1016/j.jddst.2024.106064
14. Hobbis D, Armstrong MD, Patel SH, et al. Comprehensive clinical implementation, workflow, and FMEA of bespoke silicone bolus cast from 3D printed molds using open-source resources. J Appl Clin Med Phys. 2024;25(11):e14498. https://doi.org/10.1002/acm2.14498
15. Nakamura K, Monzen H, Kubo K, et al. The development and characterization of an all-purpose bolus for radiotherapy. Phys Med Biol. 2023;68(10). https://doi.org/10.1088/1361-6560/acc7e0
16. Gugliandolo SG, Pillai SP, Rajendran S, et al. 3D-printed boluses for radiotherapy: influence of geometrical and printing parameters on dosimetric characterization and air gap evaluation. Radiol Phys Technol. 2024;17(2):347–59. https://doi.org/10.1007/s12194-024-00782-1
17. Wang KM, Rickards AJ, Bingham T, Tward JD, Price RG. Technical note: evaluation of a silicone-based custom bolus for radiation therapy of a superficial pelvic tumor. J Appl Clin Med Phys. 2022;23(4):e13538. https://doi.org/10.1002/acm2.13538

18. Lobo D, Banerjee S, Srinivas C, et al. Influence of air gap under bolus in the dosimetry of a clinical 6 MV photon beam. J Med Phys. 2020;45(3):175–81. https://doi.org/10.4103/jmp.JMP_53_20
19. Dahn HM, Boersma LJ, de Ruysscher D, et al. The use of bolus in postmastectomy radiation therapy for breast cancer: A systematic review. Crit Rev Oncol Hematol. 2021;163:103391. https://doi.org/10.1016/j.critrevonc
20. Andic F, Ors Y, Davutoglu R, Baz Cifci S, Ispir EB, Erturk ME. Evaluation of skin dose associated with different frequencies of bolus applications in postmastectomy three-dimensional conformal radiotherapy. J Exp Clin Cancer Res. 2009;28(1):41. https://doi.org/10.1186/1756-9966-28-41
21. Park SY, Choi CH, Park JM, Chun M, Han JH, Kim JI. A Patient-Specific polylactic acid bolus made by a 3D printer for breast cancer radiation therapy. PLoS ONE. 2016;11(12):e0168063. https://doi.org/10.1371/journal.pone.0168063. Published 2016 Dec 8.
22. Gul OV, Demir H, Basaran H, et al. Investigation of the effect of bolus on skin dose in breast cancer treatment with tomotherapy and LINAC radiotherapy devices. Radiat Phys Chem. 2024;218. https://doi.org/10.1016/j.radphyschem.2024.111625
23. Demir H, Gul OV, Aksu T. Investigation of skin dose of post-mastectomy radiation therapy for the halcyon and tomotherapy treatment machine: comparison of calculation and in vivo measurements. Radiat Meas. 2024;173. https://doi.org/10.1016/j.radmeas.2024.107112

Publisher's note